

Shape-Tailored Porous Gold Nanowires: From Nano Barbells to Nano Step-Cones

Rawiwan Laocharoensuk,[†] Sirilak Sattayasamitsathit,^{†,*} Jared Burdick,[†] Proespichaya Kanatharana,^{*} Panote Thavarungkul,^{*} and Joseph Wang^{†,*}

[†]BioDesign Institute, Departments of Chemical Engineering and Chemistry and Biochemistry, Arizona State University, Tempe, Arizona 85287, and ^{*}Faculty of Science, Prince of Songkla University, Hat Yai, Songkhla, 90112 Thailand

Nanowires are critically important building blocks of nanotechnology.^{1,2} An attractive and versatile route for preparing nanowires involves the electrodeposition into the cylindrical nanopores of a host porous membrane template, followed by dissolution of the template.³ Such a template-assisted electrochemical synthesis route permits a convenient and reproducible preparation of nanowires of a variety of sizes or compositions. Any material that can be electroplated can be used as a portion of the resulting nanowire. Multisegment nanowires, based on different materials, can be readily prepared by sequential electrochemical deposition of several segments (of metals, polymers, and composites), with different predetermined lengths, into the pores of the membrane template.⁴ In addition to solid metal nanowires, it is possible to prepare porous nanowires by a membrane-templated electrodeposition of a bimetallic alloy followed by the selective dissolution (de-alloying) of the less noble component.⁵ The electropolymerization of polypyrrole within the resulting nanopores led to metal/polymer composite nanowires of controllable composition.⁶ All of the above nanostructures have been characterized by a cylindrical shape of uniform diameter.

Here we report on the fabrication of shape-tailored porous gold nanowires *via* silver dissolution from multisegment gold–silver alloy nanowires with segments of different compositions. The new membrane-template protocol leads to novel step-like nanowire configurations (e.g., barbell or step-cone) containing segments with different diameters. As illustrated in Figure 1, such a protocol relies on sequentially depositing alloy segments of

ABSTRACT Step-like porous gold nanowires of different shapes and diameters have been prepared by sequentially depositing alloy segments composed of different gold/silver ratios and de-alloying the silver component. For example, step-cone and nano-barbell porous gold nanowires were generated by a membrane-templated sequential deposition of gold–silver alloy segments from plating solutions of respectively decreasing or alternating gold/silver composition ratios. Alloy segments of different gold/silver ratios, prepared by using different plating potentials, also lead to multistep nanowires. In addition to step-like nanowires, we describe the preparation of cone- and bone-shaped porous nanowires from alloy nanowires of longitudinally changing compositions, generated *via* deposition from a flowing plating solution of a continuously changing composition. Such customization of the porous gold nanostructure is attributed to the chemical removal of silver and the different extents of gold reordering from alloy segments of different compositions. The latter leads to porous gold segments of smaller diameters from silver-rich alloy segments. The new “nanomachining” concept is versatile and could be extended to nanowires of diverse shapes with a variety of properties, generating an attractive assortment of nano-hardware.

KEYWORDS: nanowires · shape · alloys · porosity · gold · configurations

different gold/silver ratios (from plating solutions of decreasing or alternating gold/silver composition ratios) and etching the silver component. Taking advantage of earlier findings reported by Liu and Searson⁷ that the diameter of single-composition nanowires decreases upon dissolution of the less noble component, we now demonstrate that changing the alloy composition (by controlling the plating conditions) allows remarkable control of the shape and dimensions of the resulting wires. The different diameters of the resulting multistep nanowires reflect the larger void spaces formed between the nanowire and the template for alloy segments with higher silver content when free gold atoms (released during the silver dissolution) diffuse toward the gold-rich center. In addition to multistep nanowires, we describe for the first time the preparation of cone- and bone-shaped porous nanowires based on

*Address correspondence to joseph.wang@asu.edu.

Received for review September 25, 2007 and accepted November 27, 2007.

Published online December 14, 2007
10.1021/nn700255x CCC: \$37.00

© XXXX American Chemical Society

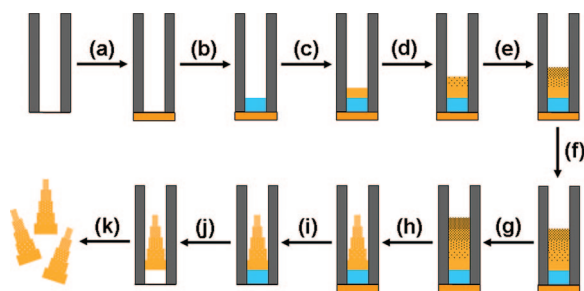


Figure 1. Scheme illustrating the template-assisted electrochemical preparation of the asymmetric porous gold nanowires: (a) sputtering gold on an alumina membrane; (b) copper deposition for a total charge of 10 C; (c) Au deposition; (d–g) deposition from Au/Ag solutions of (d) 9/1, (e) 8/2, (f) 7/3, and (g) 6/4 ratios; (h) etching the silver component using a 35% HNO_3 solution; (i) removal of the sputtered gold layer by polishing with a polishing machine and 1 μm alumina powder; (j) removal of the copper layer using 0.1 M CuCl_2 with 20% HCl ; and (k) dissolution of the membrane template using 3 M NaOH . All alloy deposition steps (d–g) were performed at -0.9 V using a charge of 0.2 C each.

gradually changing the composition of a flowing plating solution and hence the longitudinal composition of the corresponding nanowires. As will be illustrated below, such versatile tailor-made “nanomachining” results in nanoscopic objects with a wide range of shapes and dimensions.

RESULTS AND DISCUSSION

The ability to tailor the shape of porous gold nanowires and create unique and diverse stepwise nanostructures through the controlled plating of multisegment gold–silver alloy nanowires and selective silver etching is illustrated by the scanning electron micro-

scopy (SEM) and transmission electron microscopy (TEM) images in Figure 2. Such images show well-defined step-cone (A,B) and nano-barbell (C,D) porous gold nanowires. The step-cone nanostructures were prepared by sequentially depositing binary alloy segments from plating solutions of decreasing gold/silver ratios (10/0, 9/1, 8.5/1.5, 8/2, 7.5/2.5, and 7/3) to yield alloy segments containing different compositions. In contrast, the nano-barbell configurations were synthesized by alternating between plating solutions with gold/silver ratios of 9/1 and 7/3. Etching the silver component from the corresponding alloy segment results in a significant change in the diameter of the porous gold nanowire section, hence leading to distinct step-cone and barbell nanostructures. The normalized diameter of each segment of the porous gold nanostructure was calculated with respect to the diameter of the solid gold segment (bright segment in SEM and dark segment in TEM). The diameter of the step-cone porous nanowires decreased in a stepwise manner from 91% to 41% (of the pure gold segment) upon decreasing the gold/silver ratio in the plating solution from 9/1 to 7/3, respectively. In contrast, the diameter of the nano-barbell alternates reproducibly between 100% and 64% upon switching between the 9/1 and 7/3 gold/silver solutions, respectively. The diameters of each segment of the nano-barbell structure are the same when the same composition of the Au/Ag plating solution was employed. Consequently, alternating between plating solutions of high-to-low Au/Ag ratios, or in an inverse fashion, does affect the diameter of the corresponding segments and the shape of the resulting nanostructures, in general. These images confirm the ability to create step-like porous nanostructures of different shapes based on the new synthesis protocol.

Such fine and reproducible control of the diameter of the resulting porous gold segments (and hence the shape of the resulting nanostructures) reflects the different extents of gold reordering during etching of silver from alloy segments of different compositions. The de-alloying process starts when the alloy surface comes in contact with nitric acid solution. Silver atoms, connected to gold atoms in a face-centered-cubic (fcc) unit structure, are preferentially dissolved. Gold atoms with no coordination (adatoms) reorganize themselves by diffusing to a gold-rich zone and combining into a larger gold island. The atomic relocation of gold adatoms results in exposure of a new (“virgin”) alloy surface that allows the acid to penetrate toward the center and dissolve silver atoms.^{8–10} Such continuous etching of the alloy nanowires eventually creates a 3D nanoporous structure with an axially symmetric cylindrical shape (templated by the alumina membrane). Porous nanowires have been shown to decrease in diameter and increase in porosity during the initial 10 min of the etching process.⁷ Negligible changes in the porosity and diameter were observed over longer dissolution

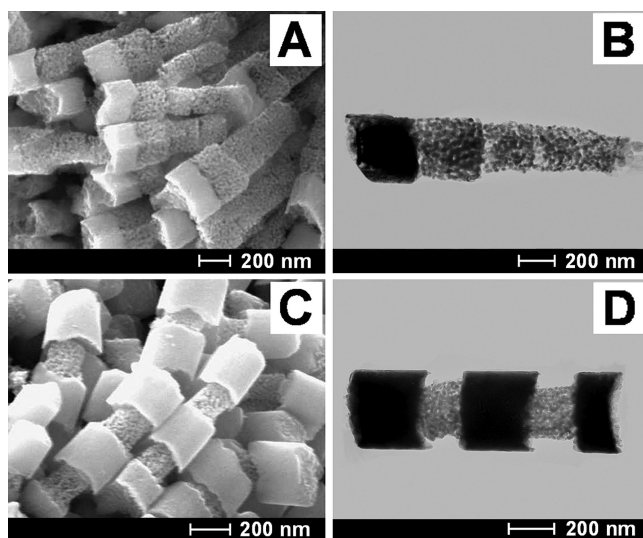


Figure 2. SEM and TEM images of multisegment asymmetric porous gold nanowires prepared at a deposition potential -0.9 V and using plating solutions of different gold/silver composition ratios. (A) SEM and (B) TEM images of the porous step-cone nanostructure prepared by plating sequentially alloy segments from plating solutions with gold/silver ratios of 10/0, 9/1, 8.5/1.5, 8/2, 7.5/2.5, and 7/3. (C) SEM and (D) TEM images of porous nano-barbell nanostructures prepared by alternating between gold/silver plating solutions of 9/1 and 7/3 composition ratios.

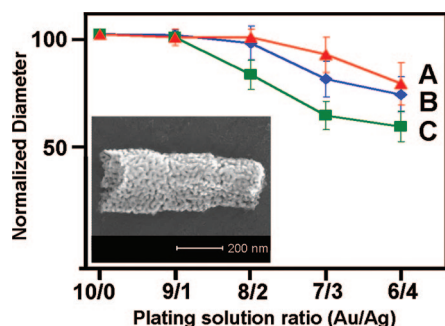


Figure 3. Normalized diameters of asymmetric porous gold nanowires obtained using different compositions of the Au/Ag plating solution (Au/Ag ratios of 10/0, 9/1, 8/2, 7/3, and 6/4) and various deposition potentials of -1.1 (A), -1.0 (B), and -0.9 V (C). The Au atom percent in the Au/Ag alloys ranged from 15% for the smallest diameter section to 85% for the largest diameter section. The normalized diameter was calculated with respect to the solid gold segment. The inset shows a SEM image of a step-cone nanowire prepared by using a 7.5/2.5 Au/Ag plating solution, with the individual alloy segments deposited at different potentials (-1.1 , -1.0 , and -0.9 V).

periods. The initial decrease of the diameter reflects the fact that free gold atoms (released from alloy during the silver dissolution) tend to diffuse toward the gold-rich center of the wire (since there is no gold on the extremities), leaving a “void space” between the nanowires and the template. Larger void spaces (*i.e.*, small outside dimensions (diameters)) are thus expected for silver-rich alloy segments. The decreased diameter of the porous gold nanowires is also in agreement with a macroscopic shrinkage of bulk Au/Ag alloy structures during electrochemical (rather than acidic) de-alloying.¹¹ The initial change in morphology (from a solid alloy to nanoporous structure) results in an increase in porosity. Yet, with sufficiently long etching times (*e.g.*, the 30 min used here), the various porous gold segments—corresponding to different alloy compositions—appear to reach a similar final density (*i.e.*, porosity), as indicated from Figure 2A,B and from additional images below. Note also (from Figure 2 and subsequent data) that alloy segments with different compositions lead to gold islands of a similar ligament size (~ 15 – 20 nm). These observations that all segments reach the same final gold density and porosity imply that “silver-rich” segments of the alloy exhibit a faster rate of gold reordering than segments with lower silver content and that the time scale for dissolution is large enough that all segments reach the same asymptotic coarsening. Consequently, alloy segments with lower gold content result in porous nanowires of smaller outside dimension.

The alloy plating potential has a profound effect upon the diameter of the resulting porous gold segments. Figure 3 displays the dependence of the normalized diameter of segments of the step-cone nanostructure upon the plating potential and the composition of the plating solution. Using a plating potential of -1.1 V, the segment diameter decreased from 100% to 78%

upon reducing the Au/Ag ratio from 9/1 to 6/4 (Figure 3A). Larger changes (reductions) in the diameter of the porous segment, down to 74% and 60% (for the 6/4 gold/silver solution), are observed using plating potentials of -1.0 V (Figure 3B) and -0.9 V (Figure 3C), respectively. This behavior reflects the different standard reduction potentials of the silver cyanide ($\text{Ag}(\text{CN})_2^-$) and gold cyanide ($\text{Au}(\text{CN})_2^-$) major components of the silver and gold plating solutions (-0.53 and -0.82 V, respectively). These result in different reduction rates of silver and gold at the different plating potentials. Searson's group¹² illustrated that the deposition current of gold starts to increase at a potential of -0.9 V and reaches its potential-independent region above -1.2 V, while that of silver is already near its plateau at -0.7 V and changes only slightly over the entire -0.7 to -1.2 V potential range. The different reduction rates lead to changes in the amount of gold plated (*i.e.*, to different alloy compositions) and, in turn, to different diameters of the corresponding nanoporous segments (after the silver dissolution). Energy-dispersive X-ray (EDX) analysis performed on the 7/3, 7.5/2.5, 8/2, and 8.5/1.5 Au/Ag segments of the alloy nanowires (grown at -0.9 V) yielded gold atom percent values of 18%, 19%, 24%, and 38%, respectively.

The profiles in Figure 3 indicate that it is possible to tailor the dimensions of the multistep nanowires by using the same plating solution while changing the deposition potential. For example, the inset in Figure 3 displays a SEM image of a step-cone porous gold nanowire prepared by using a 7.5/2.5 Au/Ag plating solution, with the individual alloy segments deposited at three different potentials (-1.1 , -1.0 , and -0.9 V). This image indicates that such stepwise electrodeposition yields a well-defined three-segment step-cone nanostructure with normalized segment diameters of 100%, 87%, and 74%. Such a multipotential single-solution protocol simplifies the preparation procedure, as it obviates the need for replacing the plating solution in connection to the different segments. Notice again the similar porosities and gold densities of the different segments of the step-cone structure (corresponding to the different alloy compositions).

It is possible also to combine the new nanomachining protocols with an electropolymerization step for preparing metal/polymer composites based on different shapes of the metal component. This can be accomplished after leaching the silver, by “backfilling” the resulting pores and surrounding gap with an electropolymerized polypyrrole while the wires are still inside the membrane template. Earlier we described a procedure for producing cylindrical (single-segment) metal/polymer composite nanowires.⁶ Figure 4 presents SEM and TEM images of a composite gold/polypyrrole nanostructure prepared by using a stepwise alloy deposition at -0.9 V from Au–Ag solutions with descending composition ratios (8.8/1.2, 8.2/1.8, and 7.8/

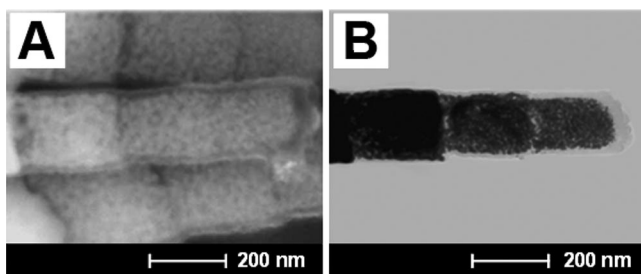


Figure 4. (A) SEM and (B) TEM images of a polymer (PPy)-covered step-cone nanowire. The porous gold step-cone was prepared by decreasing sequentially the composition of the gold in the Au/Ag mixture plating solution (Au/Ag ratios of 8.8/1.2, 8.2/1.8, and 7.8/2.2) while depositing at -0.9 V, with a 0.3 C charge for each segment. Following the silver etching, PPy was electropolymerized at $+1.2$ V for 12 s.

2.2). These images indicate that cylindrical composite nanostructures are formed with a defined internal porous gold step-cone (as in Figure 2A), but filled and surrounded with polypyrrole. This concept of metal/polymer composites can be extended to different shapes of porous gold and different polymers. Further dissolution of porous gold structure within the polypyrrole coverage could lead to porous polymer nanowires with pores reflecting the shape of the internal metal component.

In addition to step-like nanowire structures, we developed an alloy-based protocol for creating cone- and bone-shaped nanostructures based on continuously changing the composition of the Au/Ag plating solution (*i.e.*, creating alloy nanowires with a longitudinal composition gradient). Figure 5C–H demonstrates the ability to design such conical nanostructures and to tailor their diameter, length, and hence sharpness. It shows SEM and TEM images of nanocones grown by adding silver to the gold-containing growth cell at increasing flow rates of 0.37 (C,D), 1.0 (E,F) and 2.0 $\text{mL} \cdot \text{min}^{-1}$ (G,H) until a final $1:1$ Au/Ag ratio was obtained. The rate of silver addition, and thus the time needed to reach the final Au/Ag ratio ($5/5$), determines

the overall plating time and hence the final length of the nanowires. The different longitudinal composition gradients along the alloy nanowires, associated with the different silver flow rates, lead to different diameters of the nanocone porous wires (*i.e.*, to nanocones of different sharpness). For example, increasing the silver flow rates from 0.37 $\text{mL} \cdot \text{min}^{-1}$ (Figure 5C,D) to 2.0 $\text{mL} \cdot \text{min}^{-1}$ (Figure 5G,H) leads to reductions in the diameter per unit length ($\Delta d/L$) from 3% to 37% , respectively. Careful examination of these images indicates that the porosity and gold density are relatively uniform along the nanocones, analogous to earlier observations of step-cone nanowires (Figure 2).

In addition to one-directional conical nanowires, it is possible to prepare nanobone-like objects with two-directional changes. Figure 5I,J illustrates TEM and SEM images, respectively, of such nanobone porous nanowires grown by selectively adding and removing silver plating solution into a continuously flowing gold plating solution, delivered to a constant-volume (~ 1.6 mL) growth flow cell. Figure 5A,B displays the experimental setup of the growth cell. (See Methods section for more details.) The addition of silver plating solution into the gold one results in a descending Au/Ag gradient in the plating solution, leading to the first conical segment (with decreasing diameter). At the reverse point, the flow of the silver plating solution was stopped, resulting in an ascending Au/Ag concentration profile in the plating solution and in the second conical segment (with an inverse direction of diameter change). Overall, this leads to a nanobone structure with lower diameter (in the central point of reversal), corresponding to 63% of the diameter of the solid-metal sections (on both ends). The exact time-dependent composition of the Au/Ag plating solution can be determined by solving an elementary first-order differential equation for solution mixing. Such versatile use of the flow of constituents to control the time-dependent composition of the

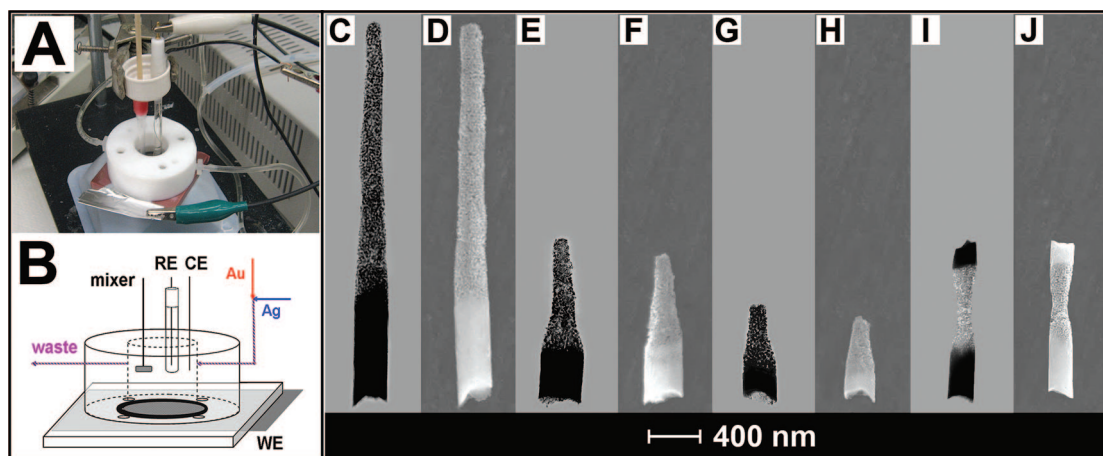


Figure 5. Nanocone (C–H) and nanobone (I,J) wires prepared by gradually changing the compositions of the plating solution. Nanocone nanowires were grown by adding 5.0 mL of silver plating solution to 5.0 mL of already present gold plating solution at varying flow rates. (C,E,G) TEM and (D,F,H) SEM images obtained using silver flow rates of 0.37 , 1.0 , and 2.0 $\text{mL} \cdot \text{min}^{-1}$, respectively. Insets (A) and (B) show the constant volume flow cell setup used to create the porous nanobone.

plating solution represents an elegant route for constructing shaped wires of different configurations.

In conclusion, we have described an attractive template-assisted electrochemical protocol for preparing shape-tailored multisegment nanowires of different shapes and diameters. This versatile shape-tailored concept can be extended to nanowires of diverse configurations with a variety of properties, based on different metals and polymers, leading to an attractive arsenal of assorted nano-hardware. The production of such shape-tailored wires could lead to wide range of potential applications, including barcoding/tagging, imaging, or de-

livery, and could have an impact in microelectronics and sensing devices. For example, the new nanomachining protocol can be used for generating barcode nanowires based on segments of different diameters and lengths, *i.e.*, of distinct shape-dependent “signatures”, analogous to the much larger lithographically prepared diameter-modulated microwires of Matthias *et al.*,¹³ leading to a wide range of tagging or multiplexed sensing applications. The tailoring of both diameter and porosity could possibly be used to tune the near-infrared absorbance of *in vivo* nanowires, aiding in pathological imaging and drug release.

METHODS

Materials. Anodisc alumina membranes with a specified pore size of 200 nm and thickness of 60 μm were purchased from Whatman (Catalog No. 6809-6022; Maidstone, UK). The pyrrole monomer was purchased from Sigma-Aldrich. The pyrrole was distilled regularly and stored at 4 $^{\circ}\text{C}$. Gold targets (used to sputter the membranes) were purchased from Denton Vacuum (Moorestown, NJ). The gold and silver plating solutions (Orotemp 24 RTU RACK, and 1025 RTU @ 4.5 Troy/gallon) were obtained from Technic Inc. (Anaheim, CA). A 161 mM pyrrole in 200 mM NaCl solution was used for electropolymerizing the polypyrrole (PPy). All other chemicals were of analytical grade purity and were used as received. All solutions were prepared using nanopure water (18 M Ω , ELGA purelab-ultra model, Ultra Scientific, Marlow, Buckinghamshire, UK).

Instrumentation. All controlled-potential experiments were performed with a CHI 621A potentiostat (CH Instruments, Austin, TX). Platinum wire and Ag/AgCl (3 M KCl, CH Instruments) served as the counter and reference electrodes, respectively. All working electrode potentials are given with respect to Ag/AgCl reference electrodes. Scanning electron microscopy (SEM) images and metal compositions were obtained with a FEI XL30 SEM instrument (FEI Co., Hillsboro, OR), equipped with an energy-dispersive X-ray analyzer (Amatek Inc., Mahwah, NJ) under an accelerating voltage of 30 kV.

Template Preparation of Multistep and Conical Nanowires. For all asymmetric nanowires, a thin film of gold was first sputtered on the branched side of the alumina membrane to provide an electrical contact for the subsequent electrochemical plating. For the asymmetric nanowires (not containing PPy), a copper base was plated first into the branched section of the membrane using a 1 M cupric sulfate pentahydrate ($\text{CuSO}_4 \cdot 5\text{H}_2\text{O}$) solution and a charge of 10 C; this was followed by 0.2 C of gold from an Orotemp 24 plating solution. Both plating steps were carried out at a potential of -0.9 V. Asymmetric gold nanowires containing PPy were grown using an initial gold base (1 C at -0.9 V), as opposed to copper and gold.

The asymmetric step-cone nanowires were prepared on top of the previously mentioned bases by sequentially depositing (at -0.9 V) alloy segments (of 0.2 C) from gold/silver plating solutions of different ratios: 9/1, 8.5/1.5, 8/2, 7.5/2.5, and 7/3 (with intermediate rinsing with nanopure water). The nano-barbells were constructed by depositing alternately (at -0.90 V) alloy segments from gold/silver mixture plating solutions with ratios of 9/1 and 7/3 for five segments of 0.2 C each (starting with the 9/1 solution). The alloy sections of the nanowires were then dealloyed with the removal of the less noble silver component by placing approximately 1 mL of a 35% (v/v) nitric acid solution in the growth cell (containing the nanowires-embedded membrane) for 15 min and then rinsing with nanopure water and repeating the process once. The membranes were then “released” from the growth cells and rinsed with nanopure water to remove all residues. After rinsing, the membranes containing copper were swabbed (on the gold-sputtered side) with a cotton-tip applicator soaked in 0.1 M CuCl_2 in 20% HCl for *ca.* 2 min. This

removed both the copper and the sputtered gold. The wires were then released from the alumina membrane as described below.

The asymmetric cone-shaped porous nanowires were constructed on the previously mentioned copper and gold bases by growing nanowires from a continuously changing Au/Ag plating solution. The solution consisted initially of 5 mL of the gold plating solution, and its composition was varied gradually by adding the silver plating solution at a fixed flow rate while plating (at -0.9 V) until obtaining a final volume of 10 mL. Different flow rates of the silver solution led to conical nanowires of different sharpnesses. Nanobone nanowires were prepared using a constant-volume growth cell setup with solution mixer. The growth cell was connected to both a 7 cm premixing tube (that delivered the plating solution) and a waste tube (that removed extraneous plating solution from the cell to maintain the total volume of *ca.* 1.6 mL). The nanobone wires were plated (at -0.9 V) from the changing solution in the growth cell. The first conical segment of the nanobone structure was deposited while flowing the silver plating solution at $0.3 \text{ mL} \cdot \text{min}^{-1}$ into a continuously flowing (at $0.7 \text{ mL} \cdot \text{min}^{-1}$) gold plating solution for 300 s. To obtain the second inverse-cone segment, the flow of silver plating solution was stopped, and only the gold plating solution was allowed to flow (at $0.7 \text{ mL} \cdot \text{min}^{-1}$) for an additional 100 s. The cone- and nanobone-containing membranes were dealloyed as described earlier for the step-cone and barbell nanowires and were released from the membrane template as described below.

The asymmetric PPy-covered step-cone nanowires were prepared atop the solid gold base by sequentially depositing at -0.9 V alloy segments of decreasing gold contents from Au/Ag solutions with descending composition ratios (87.5/12.5, 82.4/17.6, and 77.8/22.2). The silver was then removed from the alloy as aforementioned, and PPy was electropolymerized from a 160 mM pyrrole solution (in 0.2 M NaCl) for 12 s at a potential of $+1.2$ V. After removing the membrane from the growth cell and rinsing with nanopure water, the gold side of the membrane was polished with a standard 8-in. SEM sample polisher (South Bay Technology, Inc., San Clemente, CA) using 3- μm alumina powder and a Final B polishing cloth (Electron Microscopy Sciences, Washington, PA). The membrane was polished until the gold color (from the solid gold segment) on the back of the membrane was no longer visible. The wires were then released from the alumina membrane as described below.

The release of the nanowires was carried out by first thoroughly rinsing the membrane with nanopure deionized water to remove any plating solution residue. This was followed by immersing the membrane in 3 M NaOH for 10 min with only slight agitation (owing to the delicate nature of the wires). The resulting nanowire-containing NaOH solution was removed to 1.5 mL Eppendorf tubes for precipitation. Nanowires were precipitated from the solution *via* centrifugation (for 3 min at 3000 rpm) and were washed several times with nanopure water until a neutral pH was achieved. All nanowire solutions were stored at room temperature.

The diameters of the individual segments of the new nanostructures were measured from calibrated SEM images. The diameter ratio reflects the ratio of the porous gold to the solid gold segments (the latter used as 100%). For each potential (−0.9, −1.0, and −1.1 V), the data were collected from 20 step-cone wires of five segments each, where five measurements were performed on each segment for a total of 1500 measurements.

Acknowledgment. This work was supported by the National Science Foundation (Grant No. CHE 0506529). R.L. and S.S. acknowledge fellowships from the DPST Program and the Thailand Research Fund (Royal Golden Jubilee Ph.D. Program), Thailand, respectively.

REFERENCES AND NOTES

- Hurst, S. J.; Payne, E. K.; Qin, L.; Mirkin, C. A. Multisegmented One-Dimensional Nanorods Prepared by Hard-Template Synthetic Methods. *Angew. Chem., Int. Ed.* **2006**, *45*, 2672–2692.
- Wanekaya, A. K.; Chen, W.; Myung, N. V.; Mulchandani, A. Nanowire-Based Electrochemical Biosensors. *Electroanalysis* **2006**, *18*, 533–550.
- Bentley, A. K.; Farhoud, M.; Ellis, A. B.; Lisensky, G. C.; Nickel, A. M.; Crone, W. C. Template Synthesis and Magnetic Manipulation of Nickel Nanowires. *J. Chem. Educ.* **2005**, *82*, 765–769.
- Keating, C. D.; Natan, M. J. Striped Metal Nanowires as Building Blocks and Optical Tags. *Adv. Mater.* **2003**, *15*, 451–454.
- Ji, C.; Searson, P. C. Synthesis of Nanoporous Gold Nanowires. *J. Phys. Chem. B* **2003**, *107*, 4494–4499.
- Meenach, S. A.; Burdick, J.; Wang, J. Metal/Conducting-Polymer Composite Nanowires. *Small* **2007**, *3*, 239–243.
- Liu, Z.; Searson, P. C. Single Nanoporous Gold Nanowire Sensors. *J. Phys. Chem. B* **2006**, *110*, 4318–4322.
- Erlebacher, J.; Aziz, M. J.; Karma, A.; Dimitrov, N.; Sieradzki, K. Evolution of Nanoporosity In Dealloying. *Nature* **2001**, *410*, 450–453.
- Forty, A. J. Corrosion Micromorphology of Noble Metal Alloys and Depletion Gilding. *Nature* **1979**, *282*, 597–598.
- Forty, A. J.; Durkin, P. A Micromorphological Study of the Dissolution of Silver–Gold Alloys in Nitric Acid. *Philos. Mag. A* **1980**, *42*, 295–318.
- Parida, S.; Kramer, D.; Volkert, C. A.; Rösner, H.; Erlebacher, J.; Weissmüller, J. Volume Change during the Formation of Nanoporous Gold by Dealloying. *Phys. Rev. Lett.* **2006**, *97*, 035504.
- Ji, C.; Oskam, Y.; Ding, Y.; Erlebacher, J. D.; Wagner, A. J.; Searson, P. C. Deposition of $\text{Au}_x\text{Ag}_{1-x}/\text{Au}_y\text{Ag}_{1-y}$ Multilayers and Multisegment Nanowires. *J. Electrochem. Soc.* **2003**, *150*, C523–C528.
- Matthias, S.; Schilling, J.; Neilsch, K.; Müller, F.; Wehrspohn, R. B.; Gösele, U. Monodisperse Diameter-Modulated Gold Microwires. *Adv. Mater.* **2002**, *14*, 1618–1621.